

CFD DESIGN AND ANALYSIS OF A COMPACT SINGLE-SPOOL COMPRESSOR FOR A HEAVY TRANSPORT HELICOPTER'S POWERPLANT

A. Startsev*, Yu.Fokin**, Eu. Steshakov***

*****Central Institute of Aviation Motors (CIAM), Moscow, Russia *aerora@bk.ru

Keywords: thermodynamic cycle, turbo-shaft engine, axial-centrifugal compressor, CFD

Abstract

Paper concerns optimal thermodynamic cycle of 9000 HP turbo-shaft engine for a twin-engine power-plant of heavy helicopter. The cycle feasibility is approved through design of the engine core and detailed CFD design and analysis of its critical element – compressor

Paper begins with estimating the core relevant overall pressure ratio (OPR) as a trade-off between specific power and fuel consumption taking into account thermal and strength limitations. More adequately OPR is defined from considering given shaft power (SP) as a maximum work that would be obtained in expanding gas from core exit temperature and pressure to ambient pressure in an imaginary power turbine. Obtained analytical expressions are reduced to dependence between compressor efficiency (η_c) and OPR, so that optimum OPR is 18, if 82.5% compressor isentropic efficiency could be achieved.

The second part of the paper outlines detailed CFD design of the compressor. This one-spool high-speed compressor consists of a two-stage low pressure axial compressor (LPC) followed by a rear centrifugal stage – high pressure compressor (HPC).

Nomenclature

SP, HP (SHP) – shaft power, shaft horse power
CSP – core shaft power
Q – burner heat addition
OPR – overall pressure ratio
TET – turbine entry temperature

LPC – axial low-pressure compressor
HPC – centrifugal high-pressure compressor
LPC PR – pressure ratio of LPC
HPC PR – pressure ratio of HPC
CT PR – pressure ratio of core turbine
 $\eta_{c \text{ isen}}, \eta_{c \text{ poly}}$ – compressor efficiencies
 T_3 – compressor discharge temperature
 $\eta_{e \text{ isen}}, \eta_{e \text{ poly}}$ – core turbine efficiencies

1 Introduction

The modern engine's trend towards higher specific power and reduced specific fuel consumption leads to aggressive designs: fewer compressor and turbine stages, higher pressure ratio and minimal axial length of bladed rows and spacing between them.

Certainly, the next generation engine requires higher isentropic efficiency of its components. Nevertheless, actual design is a trade-off between level of complexity and component isentropic efficiency.

NASA Subsonic Rotary Wing project considers for a future 7500 and 12000 HP-class rotorcraft engines the value of cycle OPR up to 40 and turbine entry temperature (TET) equal to 3000F (1670K) (see [1]). These cycle parameters are high and cause a number of technical challengers for compressor and engine design: aerodynamics of low corrected flow in aft stages, strength-of-material and cooling limitations at high compressor discharge temperatures, two-spool architecture and other construction complexities.

A 9000 HP turbo-shaft engine considered in this paper is more conservative in OPR. The engine cycle parameters and shaft power are given in Table 1 and compared with those proposed by MTU for a similar engine (see [2]).

Table 1 Comparison of turbo-shaft engine data

	CIAM	MTU
OPR	18:1	19 – 21:1
TET	1650 K	1800 K
SP	6.6 MW	6 – 7.5 MW

Mass flow-rate equal to 22.3 kg/s has been chosen to provide 6.6 MW shaft power. Core engine includes the following components: compressor with minimum number of stages and variable stator vanes, short annular combustor and one-stage axial turbine with cooled turbine stator/rotor blades made of nickel-base alloys.

One of the core design targets is compactness and simplicity of architecture based on current level of technology (see Fig.1).

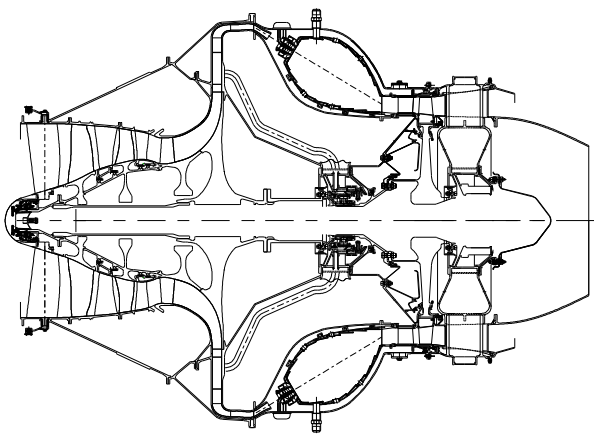


Fig.1 Core of 9000 HP turbo-shaft engine

Core is single-spool with high rotational speed. Core turbine is one-stage and supersonic. Compressor is also supersonic with only one variable stator vane (namely, LPC inlet guide vane). Stage number is minimized through axial-centrifugal configuration of compressor. Flow-path of LPC is tailored so that intermediate S-shaped duct between LPC and HPC is practically absent.

Importance of compressor design has been shown in paper [3]. Paper [3] outlines optimum

engine configurations for light and medium rotorcrafts where compressor flow-rate and LPC/HPC pressure ratios appear as the principal design variables of the engines.

Valuable overview of different compressor concepts for a small 40kW – 100kW class turbo-shaft engine has been given in [4]. Six compressor concepts have been assessed. Three stage 6.5:1 pressure ratio compressor (two axial stages and diagonal stage) has been chosen as the best configuration. It is interesting to note that two-stage axial-centrifugal compressor with the same pressure ratio has been rejected. The reason was that “aerodynamical matching between an axial stage and a radial stage requires a tuning of the blade tip speeds and thus the blade loading of both stages”.

Only few patents disclose proportion between axial stages pressure ratio (LPC PR) and centrifugal stage pressure ratio (HPC PR) of an axial-centrifugal compressor. The PWC patent [5] proposes single stage axial LPC (LPC PR equals 1.66:1, isentropic efficiency equal to 0.87) and centrifugal HPC (HPC PR equals 6.04:1 with isentropic efficiency equal to 0.829). It is interesting to note that OPR of this two-stage compressor is 10:1 and isentropic efficiency is equal to 0.82 (rather high value).

On the basis of these data, it looks reasonable to consider as optimum 1:3 ratio between LPC PR (with moderately loaded high-aspect ratio stages) and HPC PR (with high-pressure centrifugal impeller). In this case impeller discharge absolute flow is supersonic requesting careful design of radial bladed diffuser and outlet system. Returning to [4], one can read that “real aerodynamic challenge is the design of the stator of diagonal stage. The stator has to provide a very high flow turning at a high inlet Mach number. At the same time, the stator system must decrease the meridional Mach number to values around 0.2 in order to minimize the total pressure loss over the burner”. Carefully designed outlet system of centrifugal stage proposed in this paper consists of a double-row bladed diffuser, de-swirl vanes and pre-diffuser of combustion chamber. Mach number at the outlet of pre-diffuser is 0.143 (with a 3.24° flow swirl).

2 Choice of thermodynamic cycle parameters

Core engine configuration includes the following components:

- compressor with minimum number of stages and variable stator vanes
- short annular combustor
- one-stage supersonic axial turbine with cooled turbine stator and rotor blades made of nickel-base alloys.

As the initial guess for the future development the following design point parameters of core engine are given: polytropic compressor efficiency $\eta_{c\ poly} = 0.879$, combustor discharge temperature $TET=1650\ K$, turbine pressure ratio $CT\ PR= 4.3$, polytropic turbine efficiency $\eta_{e\ poly} = 0.85$.

Fig. 2 demonstrates specific power and specific fuel consumption (SFC) depending on OPR under given core engine parameters. Calculation formulas are well-known can be found in [6]).

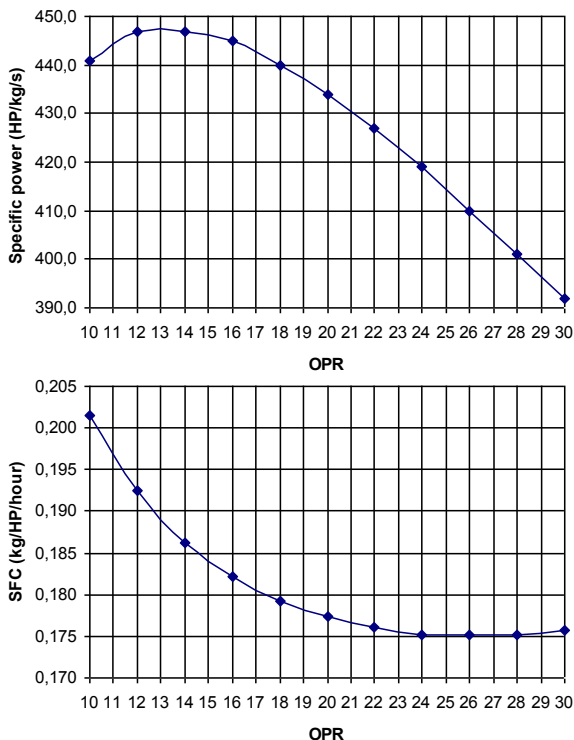


Fig.2 Specific power and SFC vs OPR

It can be seen that maximum specific power of the engine is achieved at $OPR=13:1$ and minimum specific fuel consumption is obtained at $OPR=26:1$. Note that for moderate OPR

(near 18:1) variation of SFC is already small, but specific fuel consumption still remains high. It means that 18 looks like a reasonable OPR for the core engine allowing trade-off between comparatively high specific power to confine mass flow-rate and size of compressor and fairly low SFC.

Further arguments invoked in favour of moderate value of OPR concern strength-of-material limitation of current technology level.

Table 2 shows compressor exit temperature versus OPR resulted from thermodynamic cycle calculations. The data are in line with the paper [1] considerations. Fig.3 taken from [1] demonstrates that use of centrifugal compressor as rear stage for OPR larger than 20:1 requires high strength materials.

Table 2 Compressor discharge temperature

OPR	18:1	20:1	22:1	24:1	26:1
$T_3(K)$	722	745	767	787	806
$T_3(^{\circ}F)$	840	882	921	957	991

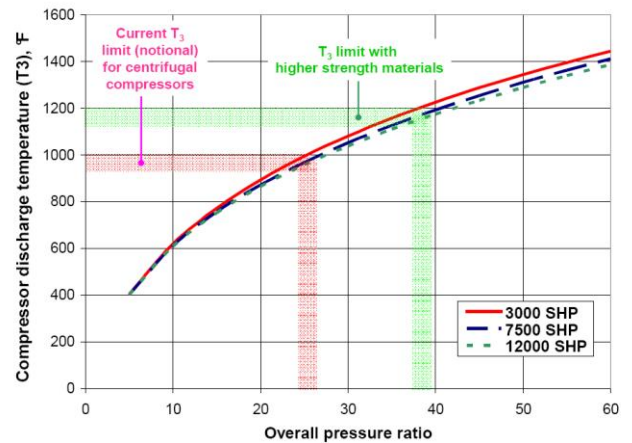


Fig. 3 Compressor exit temperature vs OPR [1].

Thus it can be concluded that a good estimation of compressor for 9000 HP engine core is a high rotational speed axial-centrifugal compressor with minimum (2+1) number of stages providing moderate values of $OPR=18$ and discharge temperature $T_3=722\ K$.

More adequately OPR is defined from considering given shaft power (SP) as a maximum work (so called “work potential”) that would be obtained in expanding gas from

core exit temperature and pressure to ambient pressure in an imaginary power turbine. This method developed in paper [15] for turbo-shaft engine summarizes the analytical relationship between shaft work delivered by power turbine and irreversibility. According to this approach “compressor is considered as two discrete flow stations wherein the average properties at the compressor entrance and exit are of interest. Work potential method can be used in conjunction with cycle analysis to estimate total loss inside the compressor and compare this to losses in other components such that the performance of the whole system can be optimized”. This method relates shaft work losses (loss in work potential) to flow irreversibilities by examining the entropy increase in the engine. As a result of [15] “an equation has been obtained which expresses the maximum possible shaft work (named below shaft power *SP*) output as a unique combination of compressor/HP turbine shaft work (named below core shaft power *CSP*) and burner heat”. This rule is taken from [15] and is presented here without derivation:

$$\frac{Q}{CpT_1} = \frac{\left(1 + \frac{CSP}{CpT_1}\right)}{\left(e^{\Delta S_{irr}/R}\right)^{\frac{\gamma}{\gamma-1}}} - \frac{CSP}{CpT_1} - 1 \quad (1)$$

To evaluate increase of entropy due to irreversibility ΔS_{irr} it is convenient to use relationship between ΔS_{irr} and polytropic efficiency η_{poly} of compression and expansion.

$$\frac{\Delta S_{irr}}{R} = \frac{1 - \eta_{poly}}{\eta_{poly}} \ln\left(\frac{P_{exit}}{P_{inlet}}\right) \quad (2)$$

If ΔS_{irr} in compressor is obtained then from (2) follows relationship between compressor polytropic efficiency $\eta_{c poly}$ and OPR.

To evaluate irreversibility ΔS_{irr} in compressor it is necessary to use as given the data obtained in a peculiar cycle calculation. Peculiarity of this calculation consists in ignoring the turbine cooling, so that value of TET will be smaller than in real core cycle and equal to 1394K.

Fig. 5 demonstrates cooling flow-rates in core turbine. Net cooling flow-rate accounts for 16.5% of compressor flow-rate.

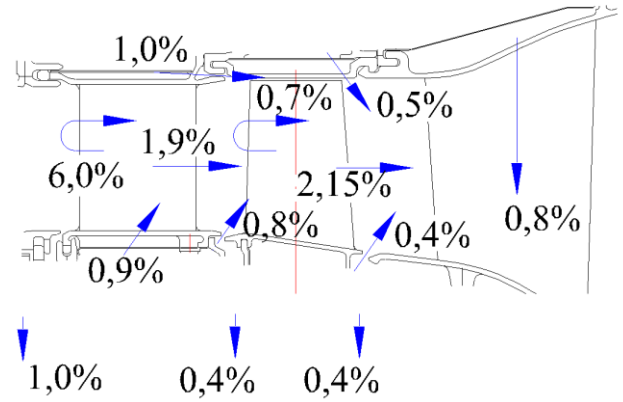


Fig 5 Distribution of cooling air in core turbine

From ambient conditions follows:

$$CpT_1 = 1007 \text{ kJ/kg/K} \cdot 288\text{K} = 290 \text{ kJ/kg}$$

From given core turbine power and flow-rate specific power of core engine can be obtained:

$$CSP = 9899.3 \text{ kW} / 22.3 \text{ kg/s} = 443.9 \text{ kJ/kg}$$

$$CSP/CpT_1 = 443.9 \text{ kJ/kg} / 290 \text{ kJ/kg} = 1.531$$

From given TET and assuming $T_3 = 722 \text{ K}$ one can obtain:

$$Q / CpT_1 = 2.338$$

Then from (1) one can obtain:

$$\Delta S_{irr}/R = 0.895$$

Design parameters of core turbine are as follows:

$$CTPR = 4.3, \eta_{e isen} = 0.865, \eta_{e poly} = 0.85$$

Then from (2) one can obtain:

$$(\Delta S_{irr}/R)_{turbine} = 0.51$$

and

$$(\Delta S_{irr}/R)_{compressor}=0.895 - 0.51= 0.385$$

Thus expression (2) is reduced to dependence between compressor efficiency (η_c) and OPR, if OPR is equal to 18, then compressor efficiencies should be no less than:

$$\eta_{c\ poly}=0.879, \quad \eta_{c\ isen}=0.825$$

3 Axial-centrifugal compressor design

For this work the following target pressure ratios have been chosen: LPC PR = 2.6:1 and HPC PR = 7:1 to obtain overall PR equal to 18:1.

To achieve target LPC PR a 2-stage LPC has been scaled from tested prototype (3-stage fan with PR equal to 4.2:1) developed earlier. Scaling coefficient is calculated to match LPC mass flow-rate requested by core. This activity specifies not only the LPC geometry but also design rotational speed of the axial-centrifugal compressor.

3D RANS performances of the prototype coincided well with experimental data obtained earlier approving validity of in-house CFD software. Design tip clearance is 0.35 mm. Geometry and performances of the 2-stage LPC are typical for high tip speed fans (see [7]). LPC rotor and stator blades are low-turning, wide-chord and of high aspect ratio. Inlet guide vane is variable (with turning flap). At the outlet of LPC the flow is axial (excluding near-hub streamlines). Tip radius of Rotor1 is 211.7 mm.

Geometry and gas-dynamics of the 1st LPC stage and 2nd stage are shown in Table 3 and 4.

Table 3. LPC. The 1st stage parameters

	Rotor1	Stator1
Hub-to-tip radius ratio	0.387	0.547
Flow Mach number Rotor tip / Stator hub	1.426	0.77
Number of blades	21	38
Solidity	1.605	1.472
Diffusion factor	0.472	0.425
Total pressure ratio	1.792	0.983

Table 4. LPC. The 2nd stage parameters

	Rotor2	Stator2
Hub-to-tip radius ratio	0.664	0.673
Flow Mach number Rotor tip / Stator hub	1.236	0.837
Number of blades	31	83
Solidity	1.563	2.081
Diffusion factor	0.398	0.354
Total pressure ratio	1.522	0.978

LPC design rotational speed is fairly high (Rotor 1 tip speed equals to 487 m/s). Together with moderate value of LPC PR it delivers rather high value of corrected rotational speed to centrifugal impeller which is good enough to obtain HPC PR = 7:1 and to design the impeller in optimal manner. Optimal design of the centrifugal stage provides high efficiency to the whole axial-centrifugal compressor. Nowadays, optimal design of a rear (high hub-to-tip diameter ratio) centrifugal stage ranks as a burning problem (see [8] and [9]).

Thus corrected flow-rate, corrected rotational speed and target HPC PR are input parameters for HPC design. Due to axial flow discharge by LPC impeller loading is obtained by its outlet geometry. HPC PR is used to determine velocity triangle at the outlet of impeller. As is known (see [10], [11]), by optimizing blade loading coupled with high impeller back-sweep angle β_{out} and increased relative velocity diffusion ratio W_{in}/W_{out} it is possible to increase centrifugal stage efficiency without compromise in HPC PR and surge margin. Large diffusion ratio means increase of blade height h_{out} at the impeller exit and diminished meridional velocity $C_{m\ out}$. Increased blade height offers the advantage of diminished relative value of tip clearance. High impeller back-sweep makes more uniform exit flow and widens range of impeller stable operation.

Paper [12] contains valuable formulae outlining the flow at the impeller outlet. Explicit formula relating variations of impeller back-sweep angle β_{out} and relative velocity diffusion ratio W_{in}/W_{out} can be derived under conditions of given (non-varied) HPC PR, tip

speed of centrifugal impeller U_{out} and outlet impeller swirl:

$$W_{in} \sin(\beta_{out}) d(W_{in}/W_{out}) + C_{m out} d(\beta_{out}) = 0 \quad (3)$$

As a result, a back-sweep $\beta_{out} = 28^\circ$, blade height $h_{out} = 20.3$ mm and tip speed of centrifugal impeller $U_{out} = 647$ m/s are adopted to obtain HPC PR=18.

Proper attention has to be given to the U_{out} . Its value has to be limited to control structural and thermal stress levels and allow currently available alloy material's application. Fig.6 taken from [13] outlines centrifugal impeller maximum allowable tip speed versus material temperature.

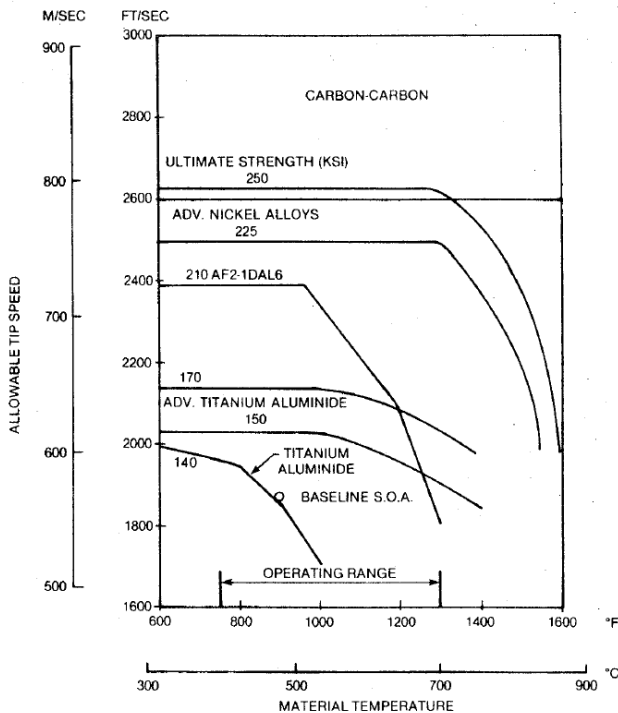


Fig. 6 Centrifugal impeller maximum allowable tip speed [12].

In our case, compressor discharge temperature is 722 K (= 450 °C) and corresponds to the left boundary of temperature operating range shown on Fig.6. As for allowable tip speed, value of 647 m/s corresponds to a titanium-base alloy. Such type titanium-base alloy is currently available.

Specified U_{out} and known compressor rotational speed give the value of impeller tip

radius R_{out} equal to 280.9 mm. At this step of impeller design it is important to specify inducer tip diameter. Below inducer tip radius is symbolized by R_{Is} .

Paper [14] explains how to choose dimensions and inlet blade angle of impeller for a given flow and pressure ratio. Formula (26) in [14] relates R_{Is}/R_{out} to the relative flow angle β_{Is} and Mach number M_{Is} at inducer tip diameter and U_{out} . Recommended by [14] value of β_{Is} is 60° . Mach number M_{Is} has to be no more than 1.25 to prevent significant shock wave losses. And using formula (26) the value $R_{Is}/R_{out} = 0.643$ has been obtained, so that $R_{Is} = 180.6$ mm.

Finally, hub radius of inducer has to be chosen to provide swallowing of given compressor mass flow-rate, so that inducer hub-to-tip radius ratio has been obtained as equal to 0.69 completing impeller design.

There is else one important question concerning intermediate S-shaped duct between LPC and HPC. Several trials are required to match LPC outlet eye and HPC inlet eye to make S-shaped duct between LPC and HPC as small as it possible. For that shroud of the LPC 2nd stage has been made descending with cylindrical hub of Stator 2.

Completion of the HPC geometry is obtained through outlet system design. Configuration of the centrifugal double-row bladed diffuser and radial-axial bend is innovative. Flow deceleration in diffuser is large, but double-row configuration inhibits advent of viscous flow separation, moreover, small total pressure loss is unprecedented. Area-controlled flow diffusion in radial-axial bend delivers low-speed uniform flow to the inlet of axial de-swirl vanes. Requested flow turning in axial de-swirl vanes is 53° . Static pressure rise coefficient of the outlet system (diffuser + de-swirl vanes) is equal to 0.84 at the total pressure recovery coefficient of 0.91.

All the HPC design efforts have been supported by 3D RANS flow simulation with 0.4 mm tip clearance in impeller. Applicability of in-house CFD software to a centrifugal stage flow simulation has been confirmed in ESPOSA project (EC FP7) by CFD calculation of high pressure ratio centrifugal compressor of

experimental AI-450S engine developed and tested by IVCHENKO-PROGRESS (Ukraine).

Gas-dynamics of the HPC impeller and double-row bladed diffuser is shown in Table 5.

Table 5. HPC. Impeller and diffuser parameters

	Impeller	Diffuser
Inlet flow angle	57.6°	77.3°
Inlet flow Mach number (Rotor tip)	1.241	1.028
Outlet flow angle	43.2°	65.6°
Outlet flow Mach number	0.382	0.289
Number of blades	14/14	21/21
Total pressure ratio	7.552	0.927

Gas-dynamics of the HPC axial de-swirl vanes and combustion chamber pre-diffuser is given in Table 6.

Table 6. HPC. De-swirl vanes and pre-diffuser parameters

	De-swirl	Pre-Diffuser
Inlet flow angle	56.1°	3.05°
Inlet flow Mach number (Rotor tip)	0.293	0.167
Outlet flow angle	3.05°	3.24°
Outlet flow Mach number	0.167	0.143
Number of blades	92	–
Total pressure ratio	0.991	0.998

After LPC and HPC design there has been made 3D viscous flow calculation through the whole axial-centrifugal compressor. As a result, Table 7 presents integral parameters of LPC stages, whole LPC, HPC and whole axial-centrifugal compressor at design point.

Table 7. Compressor integral parameters

	Total pressure ratio	Isentropic efficiency
1 st stage	1.761	0.874
2 nd stage	1.49	0.875
LPC	2.596	0.856
HPC	6.936	0.849
Whole compressor	18.0	0.826

4 Axial-centrifugal compressor geometry

Fig. 7 presents compressor dimensions. Axial length of compressor from LPC IGV leading edge to trailing edge of HPC deswirl vanes is 496.8 mm. Axial length of LPC including S-channel is 291.6 mm. Axial length of HPC impeller is 134.9 mm.

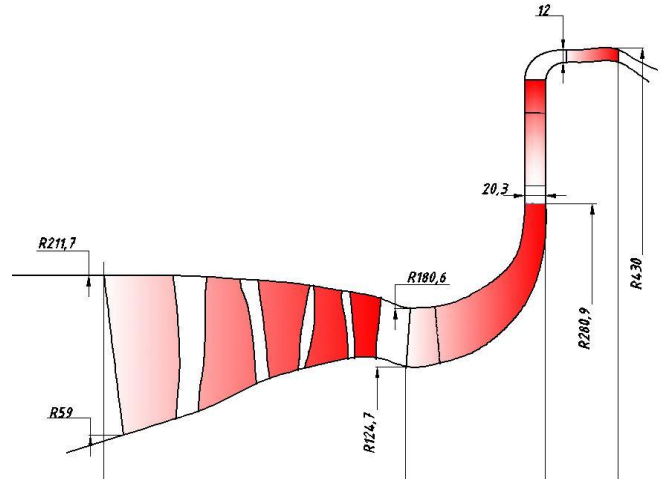


Fig. 7 Main compressor dimensions.

5 Axial-centrifugal compressor performances

After successful matching of axial LPC and centrifugal HPC stage there has been made 3D viscous flow calculation of the compressor performances for a wide range of RPM to confirm that surge margin is enough.

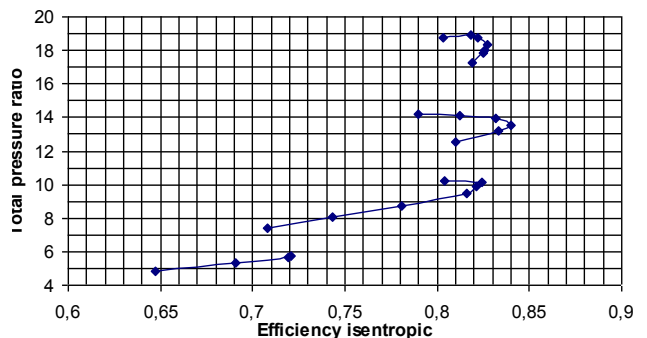
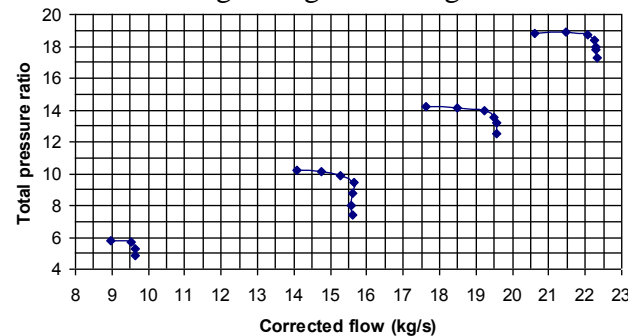


Fig.8 Axi-centrifugal compressor performances

Fig. 8 presents CFD-predicted compressor performances for the range of RPM: 100% (n=22025 RPM), 93.5%, 84.8% и 74.8%. Corresponding turning of IGV flap is as follows: 0°, 0°, 14°, 28°.

Conclusion

This paper presents CFD design and study of compact one-spool 18:1 pressure ratio axial-centrifugal compressor. High isentropic efficiency potential of the compressor (82.5%) is the main novelty of the project and essentially caused by:

- low aerodynamic loading, optimum tip speed and high flow capacity of LPC
- optimum design of centrifugal impeller
- double-row configuration of bladed diffuser
- controlled flow diffusion in radial-axial bend.

Compressor geometry and its 3D RANS performances are used as input in the core design providing basement for the 9000 HP turbo-shaft engine feasibility.

References

- [1] Welch, G.E., Hathaway, M.D., Skoch, G.J. and Snyder C.A., (2009) "Rotary-Wing Relevant Compressor Aero Research and Technology Development Activities at Glenn Research Center", American Helicopter Society 65th Annual Forum, Grapevine, TX, May 27-29, 2009.
- [2] K.Rud, (MTU), (2007), "Powerplant for Future HTH Helicopter. Advanced Engine Concepts and Technologies", 25th International Helicopter Forum, Sept 19-20, 2007.
- [3] Goulos, I., et al, (2013), "Rotorcraft Engine Cycle Optimization at Mission Level", Proceedings of ASME Turbo Expo 2013, GT2013-95678.
- [4] Kroger, G., Siller, U., Moser, T., and Hediger S., (2014), "Towards a Highly Efficient Small Scale Turboshift Engine. Part I: Engine Concept and Compressor Design", Proceedings of ASME Turbo Expo 2014, GT2014 – 26368
- [5] Stephen A. Anderson, Ronald Trumper and Gary Weir, (PWC), (2010), "Hybrid Compressor", United States Patent Application Publication No. US 2010/0232953 A1.
- [6] Kurzke, J., (2007), "About Simplifications in Gas Turbine Performance Calculations", Proceedings of ASME Turbo Expo 2007, GT2007-27620
- [7] H.E.Messenger and E.E.Kennedy, (1972), "Two-Stage Fan. Aerodynamic and Mechanical Design", NASA CR-120859.
- [8] Lurie, E.A., et al., (2011), "Design of a High Efficiency Compact Centrifugal Compressor", American Helicopter Society 67th Annular Forum, May 3-5, 2011.
- [9] Ralf von der Bank, et al, (2014), "LEMCOTEC – Improving the Core-Engine Thermal Efficiency", Proceedings of ASME Turbo Expo 2014, GT2014 – 25040.
- [10] Mileschin, V.I., Startsev, A.N., and Orekhov, I.K., (2003), "CFD Design of a 8:1 Pressure Ratio Centrifugal Compressor", Proceedings of IGTC 2003 Tokyo, Japan, November 2-7, 2003, IGTC2003Tokyo TS-043.
- [11] Takanori Shibata, et al, (2009), "Performance Improvement of a Centrifugal Compressor Stage by Increasing Degree of Reaction and Optimizing Blade Loading of a 3D-Impeller", Proceedings of ASME Turbo Expo 2009, GT2009 – 59588
- [12] Shum, Y.K.P., Tan, C.S. and Cumpsty N.A., (2000), "Impeller-Diffuser Interaction in a Centrifugal Compressor", Journal of Turbomachinery, October 2000, Vol. 122, pp. 777-786
- [13] Singh, B., (1991), "Small Engine Component Study", NASA CR-175079, Teledyne CAE Report No 2224
- [14] Daniel Rusch and Michael Casey, (2012), "The Design Space Boundaries for High Flow Capacity Centrifugal Compressors", Proceedings of ASME Turbo Expo 2012, GT2012-68105
- [15] Christofer D. Wilson, David W. Riggins, Bryce Roth and Robert McDonald, (2002), "Performance Characterization of Turboshift Engines: Work Potential and Second-Law Analysis", American Helicopter Society 58th Annular Forum, June 11-13, 2002.

Copyright Statement

The authors confirm that they, and/or their company or organization, hold copyright on all of the original material included in this paper. The authors also confirm that they have obtained permission, from the copyright holder of any third party material included in this paper, to publish it as part of their paper. The authors confirm that they give permission, or have obtained permission from the copyright holder of this paper, for the publication and distribution of this paper as part of the ICAS 2014 proceedings or as individual off-prints from the proceedings.